Dilatometric Study of the Precipitation Kinetics in Cu-Al-Ni Shape Memory Alloys

V. Recarte, R.B. Pérez-Sáez, M.L. Nó* and J. San Juan

Departamento de Física de la Materia Condensada, Facultad de Ciencias, Universidad del País Vasco, Apdo. 644, 48080 Bilbao, Spain
* Departamento de Física Aplicada II, Facultad de Ciencias, Universidad del País Vasco, Apdo. 644, 48080 Bilbao, Spain

Abstract-The maximum working temperature in CuAlNi shape memory alloys is limited by the precipitation of the stable phases that damages the good thermomechanical behaviour during the martensitic transformation. In this paper, the precipitation kinetics of the stable phases inside the metastable ß phase have been studied by quenching dilatometry in a wide range of temperatures. The different phases have been characterised by scanning electronic microscopy and X-ray diffraction. Moreover, the precipitation kinetics have been analysed using a double Jhonson-Mhell-Avrami equation. The extrapolation of the obtained characteristic parameters allows us to predict the behaviour of the alloy at lower temperatures. Finally, the TTT curve has been obtained for both the primary precipitation and the eutectoid decomposition.

1. INTRODUCTION

Among the wide variety of alloys that exhibit the shape memory effect the most developed, as a consequence of their practical applications, are the nickel-titanium alloys and the copper-based alloys such as Cu-Zn-Al and Cu-Al-Ni [1, 2]. The Cu-Al-Ni shape memory alloys have been developed as an alternative to the classically used Cu-Zn-Al and Ti-Ni alloys. The main interest of these alloys from a technological point of view is their possible use at temperatures near 200°C [3], in advantage over the Cu-Zn-Al and Ti-Ni alloys whose maximum working temperature is limited to 100°C [3] for several reasons. The main problem that must be solved to guarantee the reliability of the Cu-Al-Ni alloys at high temperatures is to determine the stability limit of both the overcooled β and the martensite metastable phases, in order to avoid the precipitation of the stable phases. During the normal use in high temperature applications, there is a critical temperature range, around 300°C, in which the alloy could be accidentally overheated, thus it is important to study the β phase stability in this temperature range.

In the present work, the stability limit of the overcooled β phase has been established by studying the precipitation kinetic curves during isothermal ageing at different temperatures between 400°C and 482°C by dilatometry. Nevertheless, the experimental study of the precipitation processes is very difficult at temperature as low as 300°C due to the extraordinarily long ageing time required to obtain the isothermal kinetics. In order to overcome this problem, the dilatometric curves have been analysed using a Jhonson-Mhell-Avrami equation, thus the microstructural parameters that control the precipitation process have been determined. This way, the TTT curves between 300°C and 482°C for the precipitation process of the stable phases have been obtained.

2. EXPERIMENTAL METHODS

Metal ingots of Cu (99.99 %), Al (99.99%) and Ni (99.97%) were melted in a high frequency induction furnace under argon atmosphere to produce an alloy ingot with a composition of Cu-13.75 Al-4.95 Ni (wt. %), analysed by plasma emission spectrometry. A Cu-Al-Ni alloy with this composition shows a double martensitic transformation linked to γ_1 and β'_1 martensitic phases [4, 5]. The obtained ingot was homogenised at 1000°C for 6 hours under argon atmosphere. The specimen of 48×6×6 mm^3 was obtained by cutting the ingot.

Conventional dilatometry at a heating-cooling rate of 4°C/min has been used to determine the transformation temperatures of the pro-eutectoid γ_1 phase (T_p=700°C), and the temperature of the eutectoid decomposition $\alpha + \gamma_1$ (T_e=575°C) [6].

The precipitation kinetics during isothermal ageing has been studied using a quenching dilatometer. An ageing process has been carried out every 12.5°C to cover the temperature range between 400°C and 482°C. Before each dilatometry measurement the sample was annealed at 900°C for 30 minutes and quenched in situ to the temperature at which the isothermal ageing was going to be carried out.

In order to characterise the phases that appear during the precipitation process, the evolution of the microstructure during the isothermal ageing has been observed by scanning electron microscopy (S. E. M.). This microscopy study has been performed in a sample which has undergone the quenching process in the dilatometer.

3. EXPERIMENTAL RESULTS AND DISCUSSION

The isothermal curves of the dilatation vs. time between 482°C and 400°C are plotted in fig. 1(a) and 1(b). They are shown in two time scales for an easier visualisation. For the same reason, the curves are normalised and vertically shifted. The curve corresponding to 450°C is represented in both figures for better comparison.
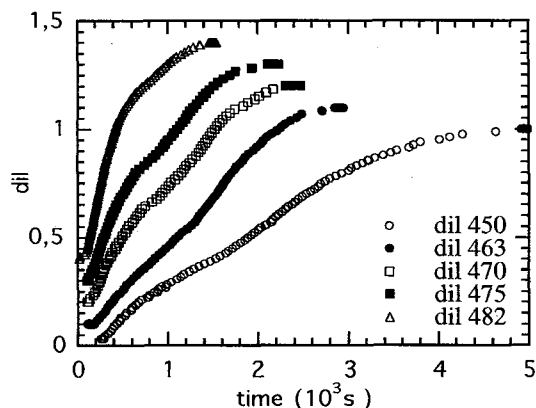

Fig. 1-a. Isothermal curves obtained by quenching dilatometry. Normalised dilatation vs. time for the temperatures between 450°C and 482°C.
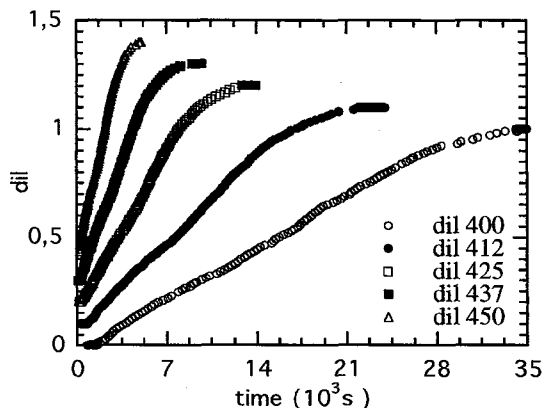
Fig. 1-b. Isothermal curves obtained by quenching dilatometry. Normalised dilatation vs. time for the temperatures between 400°C and 450°C.

In all the kinetics curves, two different stages can be clearly distinguished, each one linked to one different precipitation process. Systematic S.E.M. observations have been carried out at different times along the ageing of the sample in order to identify the two different precipitation processes. Fig. 2 shows the dilatometry curve during the isothermal precipitation at 400 °C and the S. E. M. micrographs taken at four different times :a) 50% first stage (3800 sec.), b) 90% first stage (6600 sec.), c) 50 % second stage (17700 sec.), and d) at the end of the whole ageing process. The primary precipitates, fig. 2(a), show a cuboidal shape and they are homogeneously distributed all around the matrix. The number of these precipitates increases along the evolution of their precipitation process. According to the phase diagrams proposed by R. Thomson and J. O. Edwards [7] and taking into account that the alloy is hypereutectoid, these primary precipitates have been identified as pro-eutectoid precipitates γ_1. This assumption has been verified by X-ray diffractometry [6]. It should be noted here that the γ_1 phase has been generally called γ_2 [8, 9], although we will denominate it γ_1 phase according to the last reviews [10, 11].

The micrographs taken during the second stage of the ageing process (fig. 2(c) and fig. 2(d)) allow us to identify this stage as the eutectoid $\beta \leftrightarrow \gamma_1 + \alpha$ decomposition whose typical morphology can be observed in the micrographs. This stage has been also studied by X-ray diffraction, the peaks associated to the γ_1 and α phases are clearly identified [6]. Contrary to the primary precipitation, the eutectoid
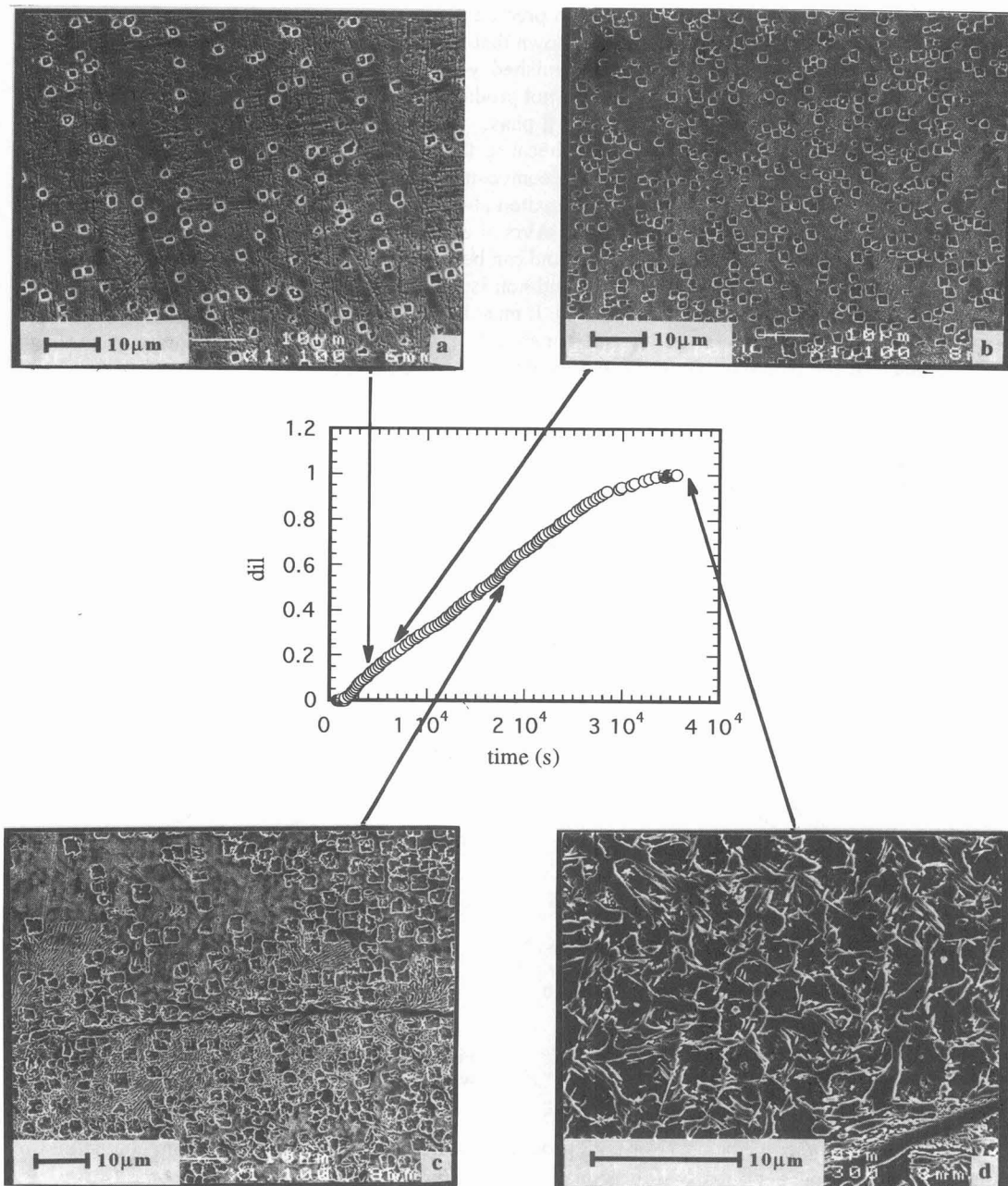
Fig. 2. S. E. M. micrographs taken at different times along the isothermal precipitation process at 400 °C. At the center of the page the experimental dilatometric curve is shown and the arrows indicate the temporal position of the micrographs:

fig. 2-a) 50 % of first stage (3800 sec.), 2-b) 90 % first stage (6600 sec.), 2-c) 50% of the second stage (17700 sec.) and 2-d) at the end of the whole precipitation process.

decomposition is heterogeneous and it starts to precipitate on the grain boundaries. In the micrograph 2(b) taken at 90 % of the first stage, it can be shown that the eutectoid decomposition has already started although the primary precipitation has not finished yet. This overlapping of the pro-eutectoid γ_1 precipitation and the eutectoid decomposition is not produced in equilibrium conditions, this behaviour is linked to the high instability of the overcooled β phase. At the end of the two stages, micrograph 2(d), the γ_1 precipitates lose their cuboidal shape because the coalescence of these precipitates with the fraction of γ_1 phase obtained by the eutectoid decomposition.

In order to obtain more quantitative information about the precipitation processes, the dilatometry curves have been fitted with the Jhonson-Mhell-Avrami equation (J-M-A) [12,13]. This equation is very useful to explain thermally activated processes and can be applied in a lot of different circumstances [14-16]. Thus, using this equation the isothermal and non isothermal kinetics of stable phases in Cu-Zn-Al shape memory alloys have been studied [17,18]. It must be remarked that in the precipitation process of the Cu-Zn-Al alloys only one stage has been analysed. In the case of this Cu-Al-Ni alloy, two stages must be analysed and then it is necessary to use a double J-M-A equation [6, 19]:

$$y = f \times \left(1 - e^{-(k_1 t)^{n_1}}\right) + (1-f) \times \left(1 - e^{-(k_2 t)^{n_2}}\right)$$

where k_i, n_i are the characteristic parameters of both precipitation processes and f is the precipitated fraction. The fit in a double J-M-A equation and the decomposition into two stages are shown in fig. 3 for the isothermal precipitation at 450°C.

Fitting all the measured dilatometry curves, the values of the characteristics parameters (n_i, k_i, f) at the different temperatures are determined. This way, taking into account that:

$$k_i = k_o e^{-E_a^{(i)}/k_b T}$$

the apparent activation energy for each stage of precipitation can be calculated from the k_1 and k_2 values.
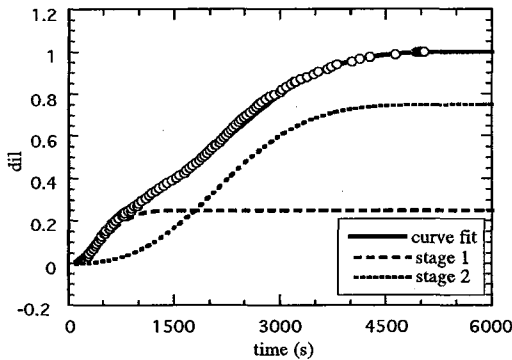

Fig. 3. Experimental data corresponding to the 450°C isothermal dilatometry and fitting to a double J.M.A. equation. Dashed lines are the decomposed single stages.
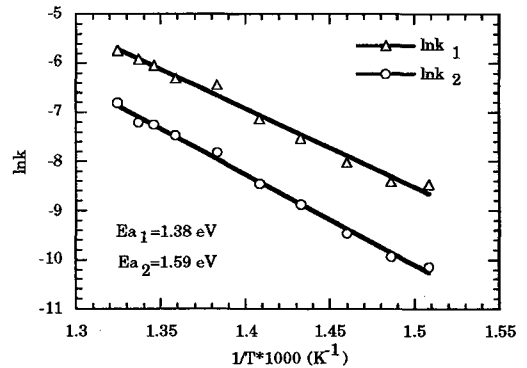
Fig. 4. Activation energies obtained from the linear regression of $ln(k)$ versus $1/T$.

Fig. 4 shows $ln(k_i)$ versus $1/T$ for both processes as well as the fit to a straight line that allows to obtain the activation energies of the primary precipitation and the eutectoid decomposition, are $E_a^{(1)} = 1.38 \pm 0.03 eV$ and $E_a^{(2)} = 1.59 \pm 0.03 eV$ respectively.

The obtained n_1 and n_2 values have been fitted by a linear regression in order to extrapolate the kinetics at low temperatures, fig. 5(a). The exponent n_1 is temperature independent, but n_2 shows a slight increase with temperature. This increase can be linked to the change of kinetic parameters when the ageing temperature approaches the eutectoid decomposition temperature Te=575°C. Because of this, only the n_2 values for the temperatures lower than 460°C have been taken for the linear fit. Fig. 5(b) shows the primary precipitation fraction f versus the ageing temperature. The f value remains practically constant below 450°C, increasing when the ageing temperature approaches the eutectoid decomposition

temperature. This is due to a decrease of the overcooling and consequently of the driving force of the eutectoid precipitation when eutectoid decomposition temperature is reached. In this way, the eutectoid fraction decreases in relation to the primary precipitation when the ageing temperature approaches the eutectoid decomposition temperature Te=575°C. The experimental values for temperatures lower than 450°C have been used to extrapolate f for low temperatures.
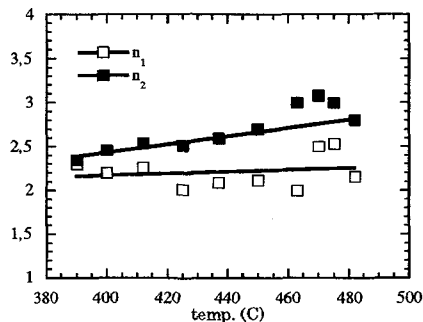

Fig. 5-a. Obtained n_1 and n_2 exponents versus temperature and the linear fits used for low temperature extrapolation.
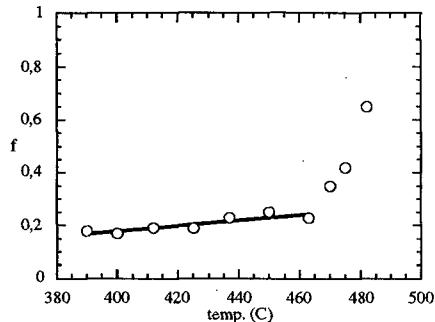

Fig. 5-b. Primary precipitation fraction f and linear fit used for low temperature extrapolation.

Once the characteristic values of both kinetics have been extrapolated for low temperatures we can generate the corresponding curves between 300°C and 400°C and determine the starting precipitation times for both processes, $\beta \leftrightarrow \gamma_1$ and $\beta \leftrightarrow \gamma_1 + \alpha$, at different temperatures. The TTT curves (for the 0.05% of both transformations) are shown in fig. 6. The line is the limit of ageing time before the beginning of the precipitation and consequently the degradation of the martensitic transformation.
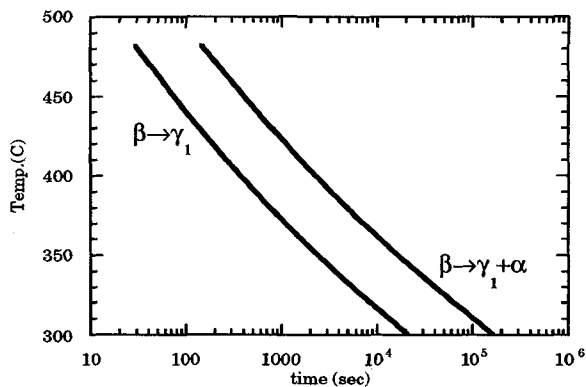

Fig 6. TTT curves of beginning of both precipitation processes obtained from their characteristic parameters.

4. CONCLUSIONS

The decomposition processes of the overcooled β phase have been studied for a Cu-Al-Ni shape memory alloy. Two successive processes have been identified, the first one the pro-eutectoid γ_1 precipitation and the second one the $\beta \rightarrow \gamma_1 + \alpha$ eutectoid decomposition. These kinetics have been fitted to a double Jhonson-Mhell-Avrami equation and the parameters of the kinetics have been obtained. By extrapolation of these parameters the kinetics at lower temperatures have been predicted. Thus we can determine the maximum using temperature before precipitation. This knowledge is very interesting in

shape memory alloys, from a technological point of view, because the working use temperature is limited by the ageing precipitation processes which damage the martensitic transformation.

References

[1]   H. Funakubo, "*Shape Memory Alloys*", Precision Machinery and Robotics Vo.1, Gordon and Breach Science Publishers, New York (1987).
[2]   "*Engineering Aspects of Shape Memory Alloys*", Ed. by T.W. Duerig, K.N. Melton, D. Stöcked and C. M. Wayman, Butterworth-Heinemann Ltd, London (1990).
[3]   L. Delaey, "Difusionless Transformation" in *Phase Transformation in Materials,*, Ed. P. Haasen, VCH, Weinheim, Germany, (1991) pp. 339-404.
[4]   V. Recarte, J. Herreros, M. L. Nó, J. San Juan; *Materials Science Forum* , **119**, 323 (1991).
[5]   V. Recarte, J. San Juan, J. Herreros, M. L. Nó; *J. de Physique IV*, **1**, C4-271 (1991).
[6]   V. Recarte, I. Hurtado, J. Herreros, M. L. Nó, J. San Juan, *Scripta Mater.*, **34**, 255 (1996).
[7]   R. Thomson, J. O. Edwards; A F S Transactions Proc. 82nd Annual Conf., **15A**, 385 (1978).
[8]   Metals Handbook, vol. 8, 8Th Edition, A. S. M., Metals Park, Ohio, U.S.A. (1978).
[9]   P. Brezina; *Int. Metals Rev.*, **27**, 77 (1982).
[10]   Binary Alloy Phase Diagrams, Ed. T. B. Massalski, A. S. M. (1986).
[11]   Ternary Alloys, vol. 4, Ed. G. Petzow and G. Effenberg, VCH,Weinheim, Germany (1991).
[12]   W. A. Jhonson, R. F. Mhel; *Trans. AIME*, **135**, 416 (1939).
[13]   M. Avrami; *J. Chem. Phys.*, 7, 1103 (1939).
[14]   J. W. Christian; "*The Theory of Transformation in Metals and Alloys*", Pergamon Press, Oxford (1975).
[15]   F. Cardellini, V. Contini, G. Mazzone; *Scripta Metall. et Mater.*, **32**, 641 (1995).
[16]   E. J. Mittemeijer, A. Van Gent, P. J. Van der Schaaf; *Metallurgical Transactions A*, **17A**, 1441 (1986).
[17]   E. S. Lee, Y. G. Kim; *Acta Metall. et Mater.*, **38**, 1669 (1990).
[18]   E. S. Lee, Y. G. Kim; *Acta Metall. et Mater.*, **38**, 1677 (1990).
[19]   V. Recarte, Ph. D. Thesis, Univ. País Vasco, Bilbao (1997).